Static FBG strain sensor with high resolution and large dynamic range by dual-comb spectroscopy

Naoya Kuse,[1,2,3,*] **Akira Ozawa,**[1,2,3] **and Yohei Kobayashi**[1,2,3]

[1]*The Institute for Solid State Physics, The University of Tokyo, 5-1-5 Kashiwanoha, Kashiwa, Chiba 277-8581, Japan*
[2]*Core Research for Evolutional Science and Technology (CREST), JST, Japan*
[3]*Exploratory Research for advanced Technology (ERATO), JST, Japan*

[*]*naoya@issp.u-tokyo.ac.jp*

Abstract: We demonstrate a fiber Bragg grating (FBG) strain sensor with optical frequency combs. To precisely characterize the optical response of the FBG when strain is applied, dual-comb spectroscopy is used. Highly sensitive dual-comb spectroscopy of the FBG enabled strain measurements with a resolution of 34 nε. The optical spectral bandwidth of the measurement exceeds 1 THz. Compared with conventional FBG strain sensor using a continuous-wave laser that requires rather slow frequency scanning with a limited range, the dynamic range and multiplexing capability are significantly improved by using broadband dual-comb spectroscopy.

© 2013 Optical Society of America

OCIS codes: (060.3735) Fiber Bragg gratings; (060.2370) Fiber optics sensors; (320.7090) Ultrafast lasers; (300.6300) Spectroscopy, Fourier transforms.

References and links

1. K. O. Hill and G. Meltz, "Fiber Bragg grating technology fundamentals and overviews," J. Lightwave Technol. **15**, 1263–1276 (1997).
2. A. D. Kersey, M. A. Davis, H. J. Patrick, M. LeBlanc, K. P. Woo, C. G. Askins, M. A. Putnum, and E. J. Friebele, "Fiber Grating Sensors," J. Lightwave Technol. **15**, 1442–1463 (1997).
3. M. Majumder, T. K. Gangopadhyay, A. K. Chakraborty, K. Dasgupta, and D. K. Bhattacharya, "Fibre Bragg gratings in structural health monitoring - Present status and applications," Sens. Actuators A. **147**, 150–164 (2008).
4. Z. He, Q. Liu, and T. Tokunaga, "Realization of nano-strain-resolution fiber optic static strain sensor for geoscience applications," CLEO 2012, **CM4B** (2012).
5. A. D. Kersey, T. A. Berkoff, and W. M. Morsey, "Multiplexed fiber Bragg grating strain sensor system with a fiber Fabry-Perot wavelength fiber," Opt. Lett. **18**, 1370–1372 (1993).
6. K. P. Koo and A. D. Kersey, "Bragg grating-based laser sensors systems with interferometric interrogation and wavelength division multiplexing," J. Lightwave Technol. **13**, 1243–1249 (1995).
7. J. H. Chow, D. E. McClelland, and M. B. Gray, "Demonstration of a passive subpicostrain fiber strain sensor," Opt. Lett. **30**, 1923–1925 (2005).
8. T. T. Y. Lam, J. H. Chow, D. A. Shaddock, I. C. M. Littler, G. Gagliardi, M. B. Gray, and D. E. McClelland, "High-resolution absolute frequency referenced fiber optic sensor for quasi-static strain sensing," Appl. Opt. **49**, 4029–4033 (2010).
9. G. Gagliardi, M. Salza, S. Avino, P. Ferraro, and P. De Natale, "Probing the ultimate limit of fiber-optic strain sensing," Science **330**, 1081–1084 (2010).
10. S. Avino, J. A. Barnes, G. Gagliardi, X. Gu, D. Gutstein, J. R. Mester, C. Nicholaou and H. P. Loock, "Musical instrument pickup based on a laser locked to an optical fiber resonator," Opt. Express **19**, 25057–25065 (2011).
11. T. T. Y. Lam, G. Gagliardi, M. Salza, J. H. Chow, and P. De Natale, "Optical fiber three-axis accelerometer based on laser locked to π phase-shifted Bragg gratings," Meas. Sci. Technol. **21**, 094010 (2010).

#185295 - $15.00 USD Received 12 Feb 2013; revised 17 Apr 2013; accepted 24 Apr 2013; published 30 Apr 2013

12. T. Udem, R. Holzwarth, and T. Hänsch, "Femtosecond optical frequency combs," Eur. Phys. J. Special Topics **172**, 69–79 (2009).
13. S. Schiller, "Spectrimetry with frequency combs," Opt. Lett. **27**, 766-768 (2002)
14. F. Keilmann, C. Gohle, and R. Holzwarth, "Time-domain mid-infrared frequency comb spectrometer," Opt. Lett. **29**, 1542–1544 (2004).
15. I. Coddington, W. C. Swann, N. R. Newbury, "Coherent dual-comb spectroscopy at high signal-to-noise ratio," Phys. Rev. A **82**, 043817 (2010).
16. I. Coddington, W. C. Swann, and N. R. Newbury, "Coherent multiheterodyne spectroscopy using stabilized optical frequency combs," Phys. Rev. Lett. **100**, 013902 (2008).
17. B. Bernhardt, A. Ozawa, P. Jacquet, M. Jacquey, Y. Kobayashi, T. Udem, R. Holzwarth, G. Guelachivili, T. W. Hänsch, and N. Picqué, "Cavity-enhanced dual-comb spectroscopy," Nature Photon. **4**, 55–57 (2010).
18. J. D. Deschênes, P. Giaccari, J. Genest, "Optical referencing technique with CW laser as intermediate oscillators for continuous full delay range frequency comb interferometry," Opt. Express **18**, 23358–23370 (2010).
19. I. Coddington, W. C. Swann, L. Nenadovic, and N. R. Newbury, "Rapid and precise absolute distance measurements at long range," Nat. Photonics **3**, 351–356 (2009).
20. I. Coddington, W. C. Swann, and N. R. Newbury, "Coherent linear optical sampling at 15 bits of resolution," Opt. Lett. **34**, 2153–2155 (2009).
21. G. Taurand, P. Giaccari, J. D. Deschênes, and J. Genest, "Time-domain optical reflectometry measurements using a frequency comb interferometer," Appl. Opt. **49**, 4413–4419 (2010).
22. T. Yasui, Y. Kabetani, E. Saneyoshi, S. Yokoyama, and T. Araki, "Tereaherz frequency comb by multi resolution terahertz spectroscopy," Appl. Phys. Lett. **88**, 241104 (2006).
23. N. Kuse, A. Ozawa, and Y. Kobayashi, "Comb-resolved dual-comb spectroscopy stabilized by free-running continuous-wave lasers," Appl. Phys. Express **5**, 112402 (2012).
24. Q. Liu, T. Tokunaga, and Z. He, "Sub-nano resolution fiber-optic static strain sensor using a sideband interrogation technique," Opt. Lett. **37**, 434–436 (2012).
25. B. R. Washburn, S. A. Diddams, N. R. Newbury, J. W. Nicholson, M. F. Yan, and C. G. Jrgensen, "Phase-locked, erbium-fiber-laser-based frequency comb in the near infrared," Opt. Lett. **29**, 250–252 (2004)

1. Introduction

Fiber Bragg gratings (FBGs) have been used as highly sensitive strain sensors [1, 2]. Strain applied to the FBG effectively deforms the Bragg grating structure, and the resulting shift in the transmission or reflection spectrum can be detected. FBG strain sensors are cost effective, small, and immune to electromagnetic interference. Therefore, they are widely used in industrial applications such as structural health monitoring and disaster detection [3].

Often FBG strain sensors are evaluated on the basis of three important characteristics: resolution, dynamic range, and multiplexing capability. Static FBG strain sensors with high resolution and high sensitivity are required in seismic and volcanic monitoring [4]. Here, "static sensor" is for the measurement of strain that changes slowly (typically below 100 Hz). The dynamic range of an FBG strain sensor is defined according to the maximal measurable strain. Multiplexing measurement, which uses multiple FBGs with different center wavelengths simultaneously, would enable efficient multipoint monitoring of strain [5, 6]. Such multiplex measurement together with a high dynamic range would provide new quantitative insights on geophysics, especially for investigating the dynamic behavior of earthquakes and volcanoes by analyzing the correlation between multiplexed FBGs. Multiplexed monitoring can also be useful for structural health monitoring because of the capability of multipoint local monitoring.

Single-longitudinal-mode continuous-wave (CW) lasers are often used to detect the spectral shift of FBGs with high resolution. In this method, the resolution is limited by the frequency noise of the laser source. Because the intrinsic noise of CW lasers is several orders of magnitude larger at low frequencies compared to that at higher frequencies, static strain sensing is more difficult than dynamic strain sensing, where a measurement frequency exceeding 100 Hz is required. In fact, for dynamic strain sensing at 100 Hz to 100 kHz, strain resolution as good as sub-pε has been already reported [7]. For static strain sensing with high resolution, stable frequency references such as Fabry-Perot cavities or frequency combs are required to stabilize the CW laser [7–9]. The fiber resonators are also used for laser stabilization, which have

#185295 - $15.00 USD Received 12 Feb 2013; revised 17 Apr 2013; accepted 24 Apr 2013; published 30 Apr 2013
(C) 2013 OSA

been applied to musical-instrument pickup [10] or fiber accelerometer [11]. Ultimate resolution cannot compete the systems in which frequency combs or stable Fabry-Perot cavities are used. However, when CW lasers are combined with Fabry-Perot cavities or frequency combs to achieve high-resolution static-strain sensing, the dynamic range and multiplexing capability are sacrificed. This is because stabilized CW lasers often have limited tunable wavelength range.

To overcome this difficulty, we focus on the use of frequency combs not as a frequency reference, but as a laser source to detect the response of FBG on account of their broad bandwidth and extremely low-frequency noise. Frequency combs can be considered as a hundred thousand ultra-low-noise CW lasers with well-calibrated frequency accuracy [12]. However, the typical frequency mode spacing is far too small to be resolved by a conventional optical spectrometer. Therefore comb-resolved characterization of FBG sensors has not been possible so far.

In this letter, we propose and demonstrate a precise and broadband characterization of FBG sensors by employing dual-comb spectroscopy [13–15]. Dual-comb spectroscopy has been applied to molecular absorption spectroscopy [15–18], distance measurement [19], characterization of fiber optics [20, 21], and THz time-domain spectroscopy [22]. When applied to FBG strain sensing, dual-comb spectroscopy enables the detection of tiny changes in the FBG spectrum in the static regime with a large dynamic range. In addition, multiple FBG sensors with different center wavelengths can be characterized simultaneously. We achieve a strain resolution of 34 nε over an optical spectrum bandwidth as wide as 1 THz. The dual-comb technique could replace conventional CW-laser-based FBG sensors, which have limited dynamic range and multiplexing capability.

2. Dual-comb spectroscopy and its application to static FBG strain sensor

In this section, we describe the basic working principles of dual-comb spectroscopy and discuss its application to a static FBG strain sensor. The output of mode-locked lasers forms a hundred thousand longitudinal modes in the frequency domain, called an optical frequency comb. Mode spacing between the combs is given by the repetition frequency (f_{rep}) of the mode-locked lasers, and the frequency of each comb mode (f_{n}) is expressed as $f_{\mathrm{n}} = f_0 + n f_{\mathrm{rep}}$, where f_0 and n are the offset frequency and integer mode number, respectively. Thus, the frequency modes can be stabilized when both offset and repetition frequencies are stabilized. A stabilized optical frequency comb serves as an ultra-precise frequency ruler and has become an indispensable tool in optical frequency metrology [12]. By interfering two frequency combs with tiny repetition frequency detuning (δ), an RF frequency beat can be obtained with multiple beat frequencies [Figs. 1(a) and 1(b)]. Those RF frequency modes have one-to-one correspondences to the optical frequency modes and therefore compose an equidistant RF comb. By measuring the RF beat signal, the optical spectrum structure can be characterized with a comb-resolved resolution. Such spectroscopy can handle a very broad optical bandwidth that is limited by the so-called aliasing effect: when an optical frequency comb broader than $\frac{f_{\mathrm{rep}}^2}{2\delta}$ is converted into the RF domain by the dual-comb method described above, more than one pair of optical frequency modes produce identical RF beat frequencies, making it impossible to uniquely determine the optical spectrum from the RF spectrum. If we set realistic values, e.g., dual-comb spectroscopy with a 100 MHz repetition frequency and a 100 Hz repetition frequency difference, an aliasing-limited bandwidth of as high as 50 THz can be obtained. Dual-comb spectroscopy can also be described in the time domain [Figs. 1(c) and 1(d)]. The timing delay between two pulses from two combs increases by $\frac{\delta}{f_{\mathrm{rep}}^2}$ over a time interval of $\frac{1}{f_{\mathrm{rep}}}$. Therefore, time-domain interference between the two combs produces a periodic pulse-like structure as shown in Fig. 1(d). By measuring the time-domain interferograms with a photo-detector and Fourier transforming the obtained time-domain signal, the optical spectrum can be reconstructed as in conventional Michelson-based

#185295 - $15.00 USD Received 12 Feb 2013; revised 17 Apr 2013; accepted 24 Apr 2013; published 30 Apr 2013
(C) 2013 OSA

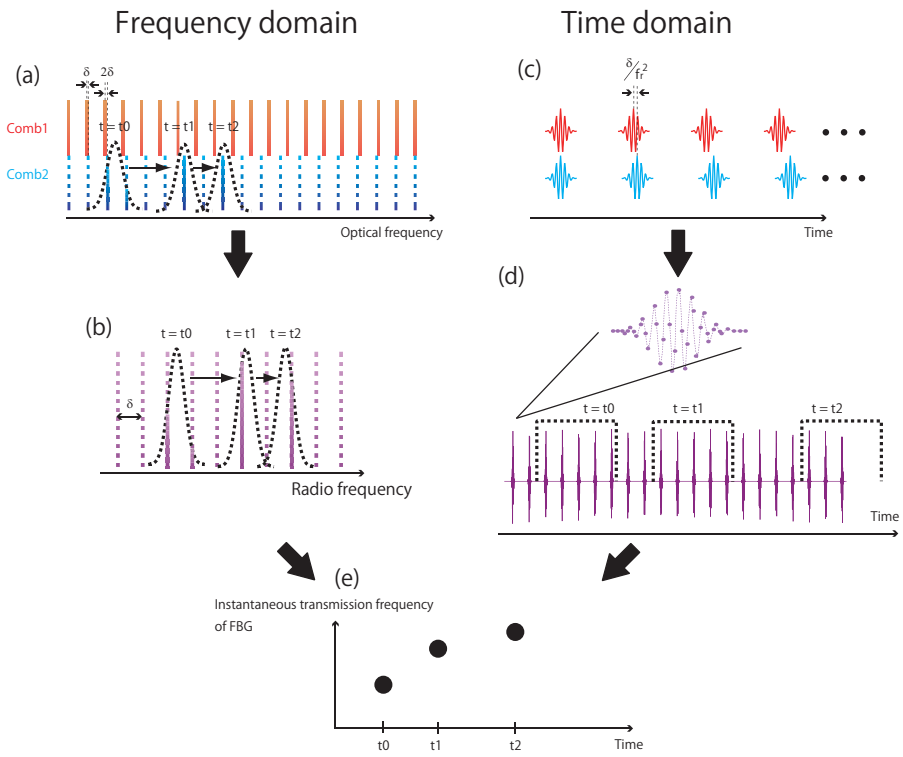

Fig. 1. Dual-comb spectroscopy and its application to FBG strain sensor. (a) Description of dual-comb spectroscopy in the frequency domain. Dotted black curve denotes time-dependent transmission spectrum of FBG. (b) RF combs obtained by interfering two combs. (c) Description of dual-comb spectroscopy in time domain. (d) Interferometric signals between two combs. Dotted black line denotes moving Fourier window. (e) Instantaneous transmission frequency of FBG.

Fourier transform spectroscopy. To apply dual-comb spectroscopy to an FBG strain sensor, an FBG can be inserted into the optical path of one of lasers, as shown in Fig. 1(a) and Fig. 2. This way, the transmission spectra of the FBGs are engraved on the RF comb.

3. Experiment

Figure 2 shows a schematic of the experimental setup. Two Yb-doped mode-locked lasers with repetition frequencies of approximately 200 MHz are used. The repetition frequency difference is set to 4.4 kHz. The two mode-locked lasers are phase locked to each other to obtain accurate interferograms. The phase-locking method used here is described in detail in reference [23]. In short, we phase-lock the two mode-locked lasers, so that one of the combs precisely follows the other, keeping the intended relationship between both the repetition and offset frequencies. The output of one laser passes through the FBG as a sample, and is spatially overlapped with the other laser to observe comb-to-comb interference. The FBG has a center frequency at 290.4 THz, and the transmission bandwidth is 500 MHz. The designed stop bandwidth is 400 GHz. The reflectivity is 70 % by design. Fiber type of the FBG is typical single-mode fiber. The FBG

#185295 - $15.00 USD Received 12 Feb 2013; revised 17 Apr 2013; accepted 24 Apr 2013; published 30 Apr 2013
(C) 2013 OSA

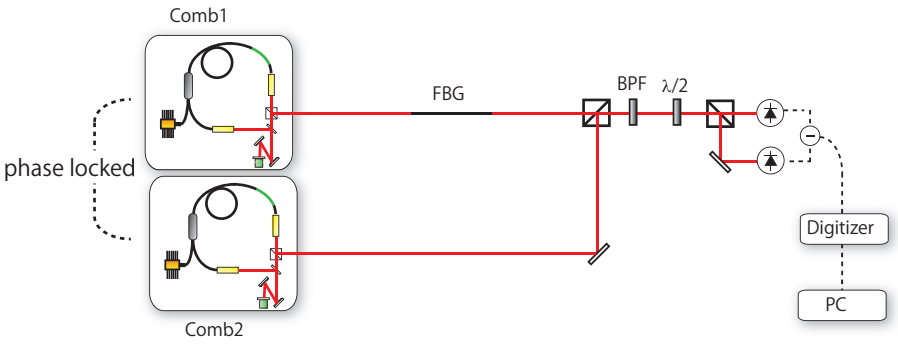

Fig. 2. Schematic of experimental setup. BPF, band-pass filter. Both frequency combs are relatively phase locked to each other. A half-wave plate is inserted to balance the power at two detectors.

is attached to a thin stainless-steel plate. A bow-like deformation is applied to the plate with a PZT actuator to strain the FBG. The band-pass filter, whose center frequency and bandwidth are 290.4 THz, and approximately 1 THz, respectively, is inserted to avoid aliasing. The overlapped beam is balance-detected to eliminate the DC component and to efficiently use the full dynamic range of the detector. A time-domain interferometric signal is digitized by a 200-MHz sampling rate by a 14-bit analog-to-digital converter. A numerical Fourier transform of the interferometric signal gives the spectrum transmitted from the FBG.

Figure 3 shows the spectra obtained with 150-ms time window for the Fourier transform. The measurement was performed without applying strain to the FBG. The obtained spectrum covers approximately 1 THz of the bandwidth. The transmission spectrum is clearly observed and agrees with the design of the FBG. In the magnified spectrum, the RF comb structure is clearly visible [Fig. 3(b)]. The linewidth of the RF combs is approximately 6 Hz in the RF domain.

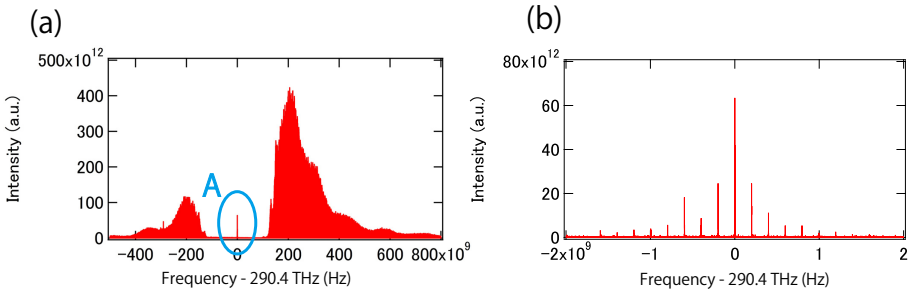

Fig. 3. Transmitted spectrum of FBG sensor without applying strain, 150-ms time window was used for Fourier transformation of time-domain interferogram. The result is shown in spans of approximately 1 THz (a), and in approximately 4 GHz (b), which is an expansion of gAh in (a).

Next, we applied the stress to the FBG by using the PZT, which pushes the base plate of the FBG, thus slightly changing the stress. This change can be observed through the transmitted wavelength shift. Figure 4(a) shows the instantaneous transmission spectra of the FBG obtained by shifting the time gate of the Fourier transform, which is called the moving-window Fourier transforming. A square window of approximately 12 ms in width is used for the moving-

#185295 - $15.00 USD Received 12 Feb 2013; revised 17 Apr 2013; accepted 24 Apr 2013; published 30 Apr 2013
(C) 2013 OSA

window Fourier transform. The transmitted optical frequency shifts gradually over some comb-mode spacings. The time dependence of the FBG's instantaneous transmission frequency can be obtained from the spectrogram. The details of the analytic method are given in the appendix, and the result is shown in Fig 4(b). The center frequency of the FBG increases continuously over the measurement time. Although linear displacement is applied to the PZT, the measured center frequency deviates from a linear slope. This is attributed to the mismatch between the movement of the PZT and that of the supporting plate because of external disturbance due to wind or fluctuation of local temperature. The mechanical resonance of the supporting plate may also affect the measurement.

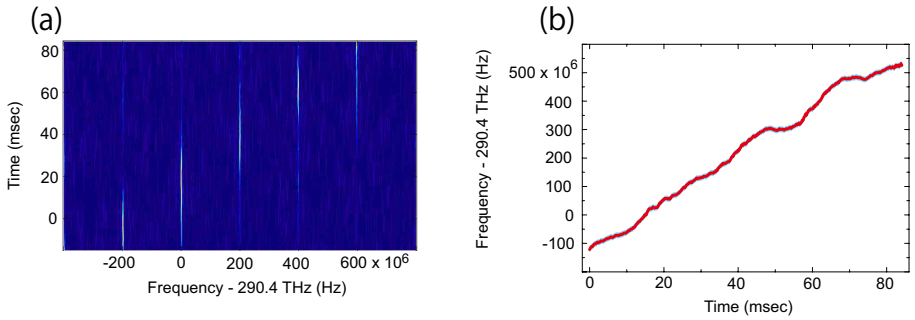

Fig. 4. (a) Instantaneous transmission spectra of FBG when linearly increasing strain is applied. The result is shown in a span of approximately 1 GHz, which corresponds to region gAh in Fig 3(a). (b) Retrieved instantaneous transmission frequency of FBG.

To evaluate the systematic error in the measurement of the FBG's center frequency, the spectrogram and instantaneous transmission frequency of the FBG were analyzed in the same way when no strain is applied. The results are shown in Fig. 5. Because a deliberate strain was not applied, the instantaneous transmission frequency should be constant. However, we observed a tiny transmission frequency fluctuation as shown in 5(b). This could be due to AM noise in the optical frequency combs, which may couple to the center frequency shift in the data analysis process. Alternatively, it could also be due to an actual change in the transmission spectrum caused by the strain applied to the FBG owing to mechanical vibration of the plate even when the PZT is kept still. We set the uncertainty of our transmission frequency determination to be the standard deviation of the center frequency fluctuation when no strain is applied to the FBG. The obtained uncertainty is 34 nε, which corresponds to an optical frequency of 10 MHz. Because some part of the center frequency fluctuation could originate from the real change in the strain as described above, we believe our evaluation gives the upper limit of the uncertainty.

4. Discussion

Applying dual-comb spectroscopy to the FBG strain senor, we demonstrate that the strain can be determined with an uncertainty as small as 34 nε over a bandwidth of 1 THz, which is limited by band-pass filtering to prevent aliasing effects. We have to point out that orders of magnitude higher resolution in strain is reported by using stabilized CW lasers [9]. Compared with those demonstration with CW lasers, much larger spectral bandwidth can be obtained with our method. Such broad-band strain detection, while maintaining high resolution, would be significantly difficult when a conventional CW method is employed. A fiber Fabry-Perot interferometers (FFPIs) with a narrow bandwidth such as a few MHz can provide enhanced frequency resolution. A FFPIs with the free spectral range of 4.1 pm and the bandwidth of 0.9 MHz is indeed available [24]. The bandwidth can also be improved by reducing the repetition frequency

#185295 - $15.00 USD Received 12 Feb 2013; revised 17 Apr 2013; accepted 24 Apr 2013; published 30 Apr 2013
(C) 2013 OSA

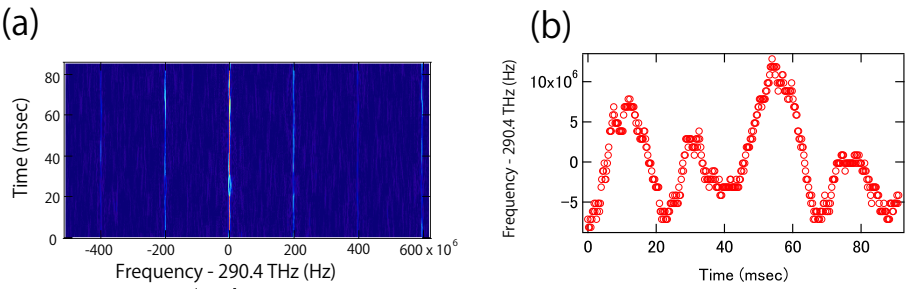

Fig. 5. (a) Instantaneous transmission spectra of FBG when no strain is applied. The result is shown in a span of approximately 1 GHz, which corresponds to region gAh in Fig 3(a). (b) Retrieved instantaneous transmission frequency of FBG. See text for details.

difference to mitigate the aliasing effect. On the other hand, our measurement with dual-comb spectroscopy is limited in measurement time upto approximately 100 ms. This is because of the long-term frequency drift of the two combs: although the two mode-locked lasers are phase-locked to each other, they can both drift synchronously for 1 MHz of optical frequency in 1 s [23]. In other words, although two frequency combs have four degrees of freedom; two offset and repetition frequencies, only two freedoms are stabilized in our phase-locking method. Thus, frequency calibration becomes impossible at longer time scales. We consider our simplified setup is sufficient for many of the applications where low frequency measurement is not necessary. However, this issue would be resolved by actively stabilizing the frequency of one of the mode-locked lasers, for example, onto a stable RF reference which is routinely done [25]. Although a 12-ms Fourier window is used in our demonstration, frequency-stabilized frequency comb enables to use longer Fourier window, which can improve the frequency resolution and the signal-to-noise ratio.

5. Conclusion

We have demonstrated a quasi-static FBG strain sensor with 34 nε-resolution and 1-THz bandwidth by dual-comb spectroscopy. This high-resolution, broad-bandwidth FBG sensor has a potential as a tool for geophysics applications.

6. Appendix

Here we illustrate the analytical process for retrieving the instantaneous center frequency of the FBG [Fig. 4(b)] from the measured data [Fig. 4(a)]. To evaluate the RF power contained in the comb-mode, each comb mode [Fig. 4(a)] is integrated around its peak [Fig. 6(a)].

$$\text{combpower}(f_n,t) = \int_{f_n-\frac{\Delta f}{2}}^{f_n+\frac{\Delta f}{2}} \text{experiment}(f,t)\,df \tag{1}$$

where f_n is the center frequency of the nth comb mode, and Δf is the integrated bandwidth (30 MHz). Further,experiment(f,t) represents the experimentally obtained data as shown in Fig. 4(a), as a function of frequency (f) and time (t).

Although the FBG spectrum in Fig. 6(a) is found to be distorted by two experimental artifacts, these artifacts can be removed to some extent as described below. One artifact is the time-varying mutual coherence between the two mode-locked lasers, which is assumed to change the instantaneous comb intensities uniformly over the entire bandwidth. Experimentally, time-varying mutual coherence between the two mode-locked lasers is due to imperfect locking

#185295 - $15.00 USD Received 12 Feb 2013; revised 17 Apr 2013; accepted 24 Apr 2013; published 30 Apr 2013
(C) 2013 OSA

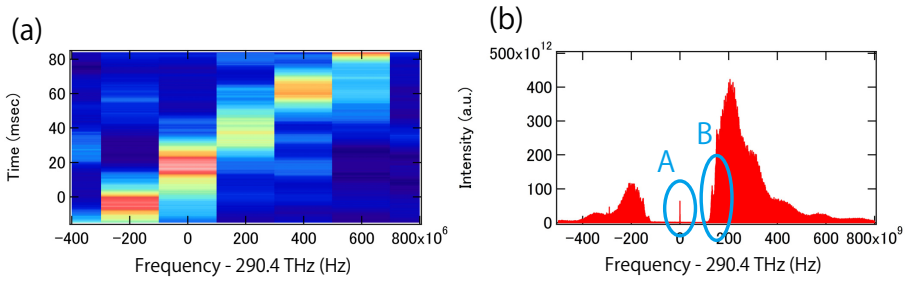

Fig. 6. (a) Power contained in the comb-mode (combpower(f_n,t)). (b) Transmission spectrum of FBG (the same as the one shown in Fig. 3(a)).

between the two combs, which is cancelled in the following way. The instantaneous spectrum in region B in Fig. 6(b) is extracted as described above [[Fig. 7(a)]. We define the value denoted as the "time-dependent coherence" as follows [Fig. 7(b)].

$$\text{coherencefunction}(t) = \frac{\sum_{n=n_B^-}^{n_B^+} \text{combpower}(f_n,t)}{n_B^+ - n_B^-} \tag{2}$$

Here, n_B^+ and n_B^- are comb number at around region "B" in Fig. 6(b) (see also Fig. 7(a)). A larger value of the "time-dependent coherence " indicates that phase locking between two-mode locked lasers works better and a high RF comb mode power is obtained. Assuming the time-

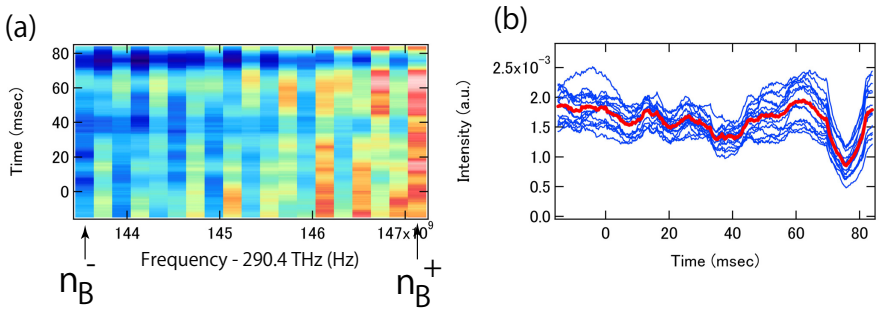

Fig. 7. (a) Power contained in the comb mode in region B of Fig. 6(b). (b) Blue curves denote combpower(f_n,t) for several n's in between n_B^+ and n_B^-. Red curve denotes coherencefunction(t).

dependent coherence is insensitive to frequency, the instantaneous comb intensities in region A in Fig. 6(b) are normalized by the time-dependent coherence.

$$\text{combpower2}(f_n,t) = \frac{\text{combpower}(f_n,t)}{\text{coherencefunction}(t)} \tag{3}$$

After this coherence correction, the peak intensity of the FBG transmission spectra should have identical values for all comb modes. However, this is not the case because of the remaining artifact of comb-mode power variation: Each comb mode power as a function of frequency (or mode number) may have mode-to-mode variation (which is expected to be constant as a function of time). The detailed process that produces this mode-to-mode power variation is not

#185295 - $15.00 USD Received 12 Feb 2013; revised 17 Apr 2013; accepted 24 Apr 2013; published 30 Apr 2013
(C) 2013 OSA

yet clear. It could be RF noise and/or already present in the original laser spectrum. To eliminate this effect, we apply the following normalization:

$$\text{combpower3}(f_n,t) = \frac{\text{combpower2}(f_n,t)}{\text{combpower2}(f_n,t_{\max,n})} \tag{4}$$

Here, $t_{\max,n}$ is the time, that maximizes combpower2(f_n,t) for a given n. After removing the two possible experimental artifacts as described above, we describe how the instantaneous center frequency of the FBG is retrieved. For a given FBG spectrum (FBG(f)), an error function is defined as follows:

$$\text{Totalerror} = \int \sum_n [\text{FBG}(f_n - f_{\text{offset}}(t)) - \text{combpower3}(f_n,t)]^2 dt \tag{5}$$

where $f_{\text{offset}}(t)$ represents the frequency shift of the FBG spectrum, which describes time dependent center frequency of the FBG. Simple multi-dimensional optimization is applied to find the best function of FBG(f) and $f_{\text{offset}}(t)$ that minimize the total error. We employed the FBG(f) that minimizes the total error as the most probable FBG spectrum.

Acknowledgments

This research was supported by the Photon Frontier Network Program of the Ministry of Education, Culture, Sports, Science and Technology (MEXT), Japan, and Research Fellowships for Young Scientists (N.K.) from the Japan Society for the Promotion of Science.

#185295 - $15.00 USD Received 12 Feb 2013; revised 17 Apr 2013; accepted 24 Apr 2013; published 30 Apr 2013
(C) 2013 OSA